



OPTIMIZATION OF A BRAYTON CYCLE AT MAXIMUM POWER OPERATING CONDITION AND AT MAXIMUM THERMAL EFFICIENCY OPERATING CONDITION

Vitor Pereira Repinaldo

Unesp/Bauru – Mechanical Engineering Department
vitor_repinaldo@hotmail.com

Santiago del Rio Oliveira

Unesp/Bauru – Mechanical Engineering Department
santiago@feb.unesp.br

Vicente Luiz Scalon

Unesp/Bauru – Mechanical Engineering Department
scalon@feb.unesp.br

Abstract. *In this work is carried out an optimization process of a Brayton power cycle for two different conditions. The first condition corresponds to the operation at full power cycle and the second condition corresponds to the operation cycle with maximum thermal efficiency. Both conditions are formulated according to the finite time thermodynamics so as to better approximate the cycle analysis of a real process. This approximation is made considering the following irreversibilities effects: thermal resistances arising from the temperature difference between the cycle and the two thermal reservoirs, heat leakage, in which part of the energy supplied by the combustion eventually is not added to the system, and the isentropic efficiencies of expansion and compression processes. Optimizations presented here are aimed to find analytical solutions for maximum power and maximum thermal efficiency according to specific conditions of the system such as the temperature of the thermal reservoirs and properties of the working fluid. Results are presented of the influence of physical parameters that affect system performance optimizations for both proposals. It is hoped that the results obtained may provide a more appropriate evaluation of real power cycles, besides being useful for projects seeking more efficient systems or systems with high power outputs.*

Keywords: *Brayton cycle, optimization, power*

1. INTRODUCTION

The Brayton cycle is an ideal model of thermodynamics cycle widely used in the representation of gas power systems, which are used both in transport application as well as in stationary power generation, and may, in the latter case, be operating together with steam power plants for electricity production, even having the advantage to offer weight and size reduced when compared to steam systems.

However, the utilization of these ideal models started to be questioned due to the existent lack between them and the real thermal cycles. Therefore, as the field of thermodynamic has been developing proposals began to emerge to make the analysis of these models closer to the operation of real heat engines. With this, it began to emerge a new branch in the thermal area which started to be recognized as finite-time thermodynamics.

Curzon e Ahlborn (1975) proposed a new evaluation method of a reversible Carnot cycle based in the fact that the maximum thermal efficiency of a heat engine operating between two thermal reservoirs with temperatures T_H and T_L , given by $\eta_{Carnot} = 1 - T_L/T_H$ would be inconsistent with the operation of real heat engines and, therefore, would be a operation limit too idealized. The authors also paid attention to the fact that for a heat engine achieve such efficiency the temperatures of the working fluid under the heat addition and heat rejection processes should be the same as the temperatures of the reservoirs. For such condition could be achieved the time required for these thermal exchanges would tend to infinity, so producing a finite quantity of work, but with the cycle operating so slowly that it would make its power output tended to zero. Thus, modeling a reversible Carnot cycle with a finite temperature difference between the thermal reservoirs and the working fluid it was found that the cycle efficiency operating under maximum power conditions is equal to $1 - \sqrt{T_L/T_H}$. For this type of model, where the only irreversibilities are the temperature difference between the reservoirs and the working fluid, was given the name of endoreversible cycle.

Using the same principle, Wu (1988, 1991) realized an optimization of an endoreversible Carnot cycle and of an endoreversible Brayton cycle developing for both an analytical expression for the power output and optimizing it numerically. Ibrahim *et al.* (1991) also optimized the power output of Carnot and Brayton cycles considering both the cases where the heat capacities of the reservoirs are infinite as in the case they are finite. Wu e Kiang (1991,1992) studied the influence of the non-isentropic compression and expansion in the efficiency of a Brayton cycle operating

under maximum power and showed that the inclusion of internal irreversibilities in the endoreversible Carnot cycle proposed by Curzon e Ahlborn (1975) could be done by a single parameter.

The study of the effects of thermal resistance, heat leakage and internal irreversibilities in the performance of a heat engine, along with the optimization of the thermal efficiency and the power output, was presented by Chen (1994) and Chen *et al.* (1997).

The analysis of an endoreversible Brayton cycle done by Chen *et al.* (2002) compared the results obtained from the optimization of the power output with those obtained by the optimization of the power density, the ratio between the power output and the maximum specific volume of the cycle.

Zhang *et al.* (2009) optimized a Brayton cycle coupled with a reverse Brayton cycle considering several types of losses found in real heat engines and Sánchez-Orgaz *et al.* (2010) presented a general model for a multi-step regenerative and irreversible Brayton cycle with reheating between the turbines and intercooling between the compressors obtaining relations for maximum power and maximum efficiency. Zhang *et al.* (2012) analyzed and optimized the arrangement of a regenerative Brayton cycle parallel to two inverse Brayton cycles where the regeneration process occurs before the inverse cycles. Analytical expressions for the efficiency and the power output was obtained and optimized.

In this paper is presents the development, analysis and comparison between the optimization of the power output and thermal efficiency of a Brayton cycle considering several types of irreversibilities found in real heat engines, such as the thermal resistances arising from the temperature difference between the cycle and the two thermal reservoirs, heat leakage, in which part of the energy supplied by the combustion eventually is not added to the system, and the isentropic efficiencies of expansion and compression processes.

2. THERMODYNAMIC ANALYSIS

A Brayton cycle with internal irreversibilities operating at steady state between a reservoir with a high temperature T_H and a reservoir with a low temperature T_L , both with infinite heat capacities, is showed in Fig. 1(a). The process 1-2 is an isobaric heat addition and the 2-3s an isentropic expansion, while the process 2-3 is a non-isentropic expansion considering the irreversible nature of real turbines. In the process 3-4 there is an isobaric heat rejection and in 4-1s occurs the isentropic compression, being the process 4-1 the non-isentropic compression found in real compressors.

In the power plant model of Fig. 1(b) the rate of heat transfer absorbed by the working fluid at high temperature receives the name of \dot{Q}_{HC} , while \dot{Q}_{LC} is the rate of heat rejection from the working fluid to the reservoir at low temperature. It is considered the existence of a rate of heat leakage \dot{Q}_l between the two reservoirs, with \dot{Q}_H , the total rate of heat transfer provided by the high temperature reservoir, being the sum of \dot{Q}_{HC} plus \dot{Q}_l , and the total rate of heat transfer rejected to the low temperature reservoir \dot{Q}_L the sum of \dot{Q}_{LC} plus \dot{Q}_l .

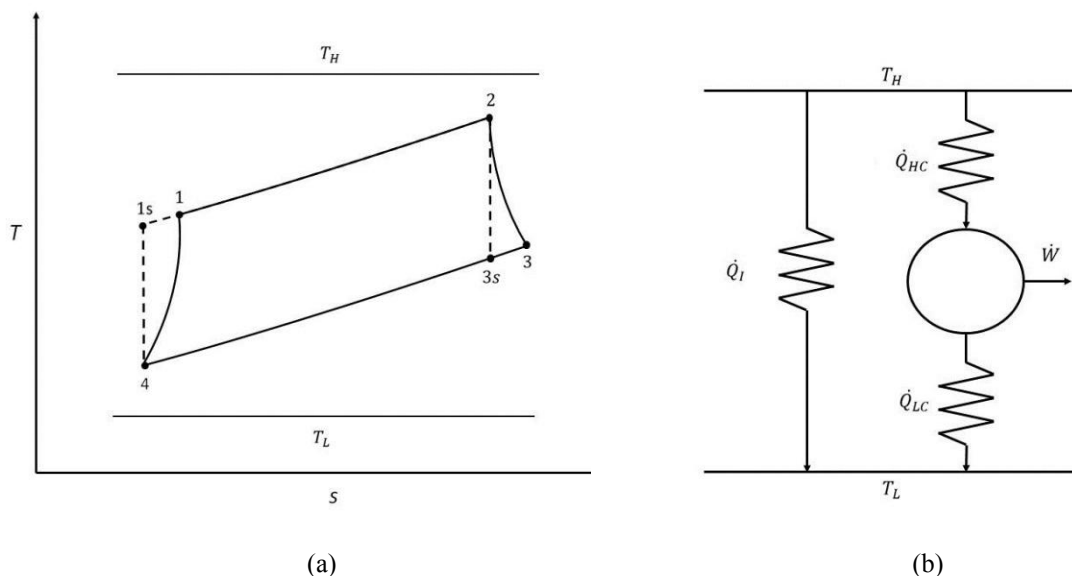


Figure 1. (a) T - s diagram of Brayton cycle (b) power plant model with heat leakage and temperature difference between the reservoirs and the heat engine.

Thus, the total rates of heat transfer provided by the hot reservoir and rejected to the cold reservoir are given, respectively, by:

$$\dot{Q}_H = \dot{Q}_{HC} + \dot{Q}_l \quad (1)$$

$$\dot{Q}_L = \dot{Q}_{LC} + \dot{Q}_l \quad (2)$$

Each of the heat transfer processes acting on the working fluid can be also calculated by the effectiveness ε of the heat exchangers as follows:

$$\dot{Q}_{HC} = \dot{C}_w(T_2 - T_1) = \dot{C}_w \varepsilon_H (T_H - T_1) \quad (3)$$

$$\dot{Q}_{LC} = \dot{C}_w(T_3 - T_4) = \dot{C}_w \varepsilon_L (T_3 - T_L) \quad (4)$$

where \dot{C}_w is the heat capacity rate of the working fluid. The heat leakage rate is given by:

$$\dot{Q}_l = \dot{C}_l (T_H - T_L) \quad (5)$$

where the factor \dot{C}_l is the rate of heat transfer between the two reservoirs per unit temperature for calculating the heat leakage. The effectiveness ε of the heat exchangers, considered countercurrents, in the hot side and in the cold side are given, respectively, by:

$$\varepsilon_H = 1 - \exp(-N_H) \quad (6)$$

$$\varepsilon_L = 1 - \exp(-N_L) \quad (7)$$

with the number of transfer units N_H and N_L being calculated as:

$$N_H = U_H A_H / \dot{C}_w \quad (8)$$

$$N_L = U_L A_L / \dot{C}_w \quad (9)$$

where U_H and U_L are the overall heat transfer coefficients of the hot and cold reservoirs, respectively. From Eq. (3) and Eq. (4) yields:

$$T_2 = \varepsilon_H T_H + (1 - \varepsilon_H) T_1 \quad (10)$$

$$T_4 = \varepsilon_L T_L + (1 - \varepsilon_L) T_3 \quad (11)$$

From the first law of thermodynamics for cycles, the power output of the cycle is given by:

$$\dot{W} = \dot{Q}_{HC} - \dot{Q}_{LC} = \dot{C}_w \varepsilon_H (T_H - T_1) - \dot{C}_w \varepsilon_L (T_3 - T_L) \quad (12)$$

Isolating T_3 from Eq. (12) yields:

$$T_3 = \frac{\varepsilon_H}{\varepsilon_L} T_H + T_L - \frac{\varepsilon_H}{\varepsilon_L} T_1 - \frac{1}{\dot{C}_w \varepsilon_L} \dot{W} \quad (13)$$

Substitution of Eq. (13) into Eq. (11) yields:

$$T_4 = \frac{\varepsilon_H (1 - \varepsilon_L)}{\varepsilon_L} T_H + T_L - \frac{\varepsilon_H (1 - \varepsilon_L)}{\varepsilon_L} T_1 - \frac{(1 - \varepsilon_L)}{\dot{C}_w \varepsilon_L} \dot{W} \quad (14)$$

The non isentropic efficiencies of the compressor and turbine are given, respectively, by:

$$\eta_c = \frac{T_{1s} - T_4}{T_1 - T_4} \quad (15)$$

$$\eta_T = \frac{T_2 - T_3}{T_2 - T_{3s}} \quad (16)$$

leading to:

$$T_{1s} = T_4 + \eta_c(T_1 - T_4) \quad (17)$$

$$T_{3s} = T_2 - \frac{(T_2 - T_3)}{\eta_T} \quad (18)$$

Substitution of Eq. (14) into Eq. (17) and Eqs. (10) and (13) into Eq. (18) yields:

$$T_{1s} = (1 - \eta_c) \left(\frac{\varepsilon_H(1 - \varepsilon_L)}{\varepsilon_L} T_H + T_L - \frac{\varepsilon_H(1 - \varepsilon_L)}{\varepsilon_L} T_1 - \frac{(1 - \varepsilon_L)}{\dot{C}_w \varepsilon_L} \dot{W} \right) + \eta_c T_1 \quad (19)$$

$$T_{3s} = \left(1 - \frac{1}{\eta_T} \right) \left[\varepsilon_H T_H + (1 - \varepsilon_H) T_1 \right] + \left(\frac{\varepsilon_H}{\varepsilon_L} T_H + T_L - \frac{\varepsilon_H}{\varepsilon_L} T_1 - \frac{1}{\dot{C}_w \varepsilon_L} \dot{W}_1 \right) / \eta_T \quad (20)$$

The following relation is obtained from the second law of thermodynamics:

$$T_{1s} T_{3s} = T_2 T_4 \quad (21)$$

The substitution of Eqs. (10), (14), (19) and (20) into Eq. (21) finally gives:

$$a_1 \dot{W}^2 + a_2 \dot{W} + a_3 = 0 \quad (22)$$

where:

$$a_1 = (1 - \varepsilon_L)(1 - \eta_c) \quad (23)$$

$$a_2 = b_1 T_1 + b_2 \quad (24)$$

$$a_3 = b_3 T_1^2 + b_4 T_1 + b_5 \quad (25)$$

$$b_1 = \left\{ (\varepsilon_H - 1) [1 - (1 - \eta_T) \eta_c] \varepsilon_L^2 + [((3 - \eta_T) \varepsilon_H + \eta_T - 2) \eta_c + 1 - 3\varepsilon_H] \varepsilon_L + 2(1 - \eta_c) \varepsilon_H \right\} \dot{C}_w \quad (26)$$

$$b_2 = [((1 - \eta_T) \eta_c - 1) \varepsilon_H T_H + (1 - \eta_c) T_L] \varepsilon_L^2 \dot{C}_w + [(3 - (3 - \eta_T) \eta_c) \varepsilon_H T_H - 2(1 - \eta_c) T_L] \varepsilon_L \dot{C}_w - 2(1 - \eta_c) \varepsilon_H T_H \dot{C}_w \quad (27)$$

$$b_3 = (\varepsilon_H \varepsilon_L - \varepsilon_H - \varepsilon_L) \left\{ [(1 - (1 - \eta_T) \eta_c) \varepsilon_H + (1 - \eta_T) \eta_c] \varepsilon_L - (1 - \eta_c) \varepsilon_H \right\} \dot{C}_w^2 \quad (28)$$

$$b_4 = ((T_L - \varepsilon_H T_H) \varepsilon_L + \varepsilon_H T_H) \left\{ [(1 - (1 - \eta_T) \eta_c) \varepsilon_H + (1 - \eta_T) \eta_c] \varepsilon_L - (1 - \eta_c) \varepsilon_H \right\} \dot{C}_w^2 + (\varepsilon_H \varepsilon_L - \varepsilon_H - \varepsilon_L) \left\{ [(1 - \eta_T) \eta_c - 1] \varepsilon_H T_H + (1 - \eta_c) T_L \right\} \varepsilon_L + (1 - \eta_c) \varepsilon_H T_H \dot{C}_w^2 \quad (29)$$

$$b_5 = [(1 - (1 - \eta_T) \eta_c) \varepsilon_H \varepsilon_L T_H - (1 - \eta_c) (\varepsilon_L T_L + \varepsilon_H T_H)] \left\{ (\varepsilon_H T_H - T_L) \varepsilon_L - \varepsilon_H T_H \right\} \dot{C}_w^2 \quad (30)$$

Thus, there was obtained a second degree polynomial for the power output of the Brayton cycle as a function of the temperature of a single state of the cycle, which is the compressor exit temperature T_1 :

Vitor Pereira Repinaldo, Santiago del Rio Oliveira, Vicente Luiz Scalon
Optimization of a Brayton Cycle at Maximum Power Operating Condition and at Maximum Thermal Efficiency Operating Condition

$$\dot{W} = \frac{-a_2 - \sqrt{a_2^2 - 4a_1a_3}}{2a_1} = \frac{-b_1T_1 - b_2 - \sqrt{(b_1T_1 + b_2)^2 - 4a_1(b_3T_1^2 + b_4T_1 + b_5)}}{2a_1} \quad (31)$$

3. POWER OUTPUT OPTIMIZATION

The maximization of \dot{W} as a function of T_1 can be done through the operation $\partial\dot{W}_1/T_1 = 0$ utilizing Eq. (31) to obtain the following expression:

$$b_6T_1^2 + b_7T_1 + b_8 = 0 \quad (32)$$

where:

$$b_6 = b_1^2b_3 - 4a_1b_3^2 \quad (33)$$

$$b_7 = 2b_1b_2b_3 - 4a_1b_3b_4 \quad (34)$$

$$b_8 = b_1b_2b_4 - a_1b_4^2 - b_1^2b_5 \quad (35)$$

The optimum temperature for the power output maximization is then given by:

$$T_{1,\dot{W}} = \frac{-b_7 - \sqrt{b_7^2 - 4b_6b_8}}{2b_6} \quad (36)$$

where \dot{W}_{\max} and the optimum temperatures $T_{1,\dot{W}}$, $T_{1,\dot{W}}$ and $T_{1,\dot{W}}$ for the cycle to operate at maximum power can be calculated substituting Eq. (36) into Eqs. (31), (10), (13) e (14). Likewise, the rates of heat transfer can be obtained substituting the values of the optimum temperatures into Eqs. (1) to (4). Lastly, expressions for the entropy generation rate $\dot{S}_{g,\dot{W}}$ and for the thermal efficiency $\eta_{\dot{W}}$ at maximum power condition are written as:

$$\dot{S}_{g,\dot{W}} = \frac{\dot{Q}_{L,\dot{W}}}{T_L} - \frac{\dot{Q}_{H,\dot{W}}}{T_H} = \frac{\dot{Q}_{LC,\dot{W}} + \dot{Q}_I}{T_L} - \frac{\dot{Q}_{HC,\dot{W}} + \dot{Q}_I}{T_H} \quad (37)$$

$$\eta_{\dot{W}} = \frac{\dot{W}_{\max}}{\dot{Q}_{H,\dot{W}}} = \frac{\dot{W}_{\max}}{\dot{Q}_{HC,\dot{W}} + \dot{Q}_I} \quad (38)$$

4. THERMAL EFFICIENCY OPTIMIZATION

The thermal efficiency η can be written as:

$$\eta = \frac{\dot{W}}{\dot{Q}_H} = \frac{\dot{W}}{b_9T_1 + b_{10}} \quad (39)$$

where:

$$b_9 = -\dot{C}_w \varepsilon_H \quad (40)$$

$$b_{10} = \dot{C}_w \varepsilon_H T_H + \dot{C}_I (T_H - T_L) \quad (41)$$

The maximization of η is obtained in a similar manner to the power output maximization substituting Eq. (31) into Eq. (39) and making $\partial\eta/\partial T_1 = 0$. This operation yields to:

$$b_{11}T_1^2 + b_{12}T_1 + b_{13} = 0 \quad (42)$$

where:

$$b_{11} = b_1^2 b_3 b_{10}^2 - 4a_1 b_3^2 b_{10}^2 + 4a_1 b_3 b_4 b_9 b_{10} + b_1 b_2 b_4 b_9^2 - b_2^2 b_3 b_9^2 - a_1 b_4^2 b_9^2 - b_1^2 b_4 b_9 b_{10} \quad (43)$$

$$b_{12} = 2b_1 b_2 b_3 b_{10}^2 + 2a_1 b_4^2 b_9 b_{10} + 8a_1 b_3 b_5 b_9 b_{10} - 2b_2^2 b_3 b_9 b_{10} - 2b_1^2 b_3 b_9 b_{10} - 4a_1 b_3 b_4 b_7^2 - 4a_1 b_4 b_5 b_6^2 + 2b_1 b_2 b_5 b_6^2 \quad (44)$$

$$b_{13} = -4a_1 b_5^2 b_9^2 - b_1^2 b_5 b_{10}^2 + 4a_1 b_4 b_5 b_9 b_{10} - b_2^2 b_4 b_9 b_{10} - a_1 b_4^2 b_{10}^2 + b_1 b_2 b_4 b_{10}^2 + b_2^2 b_3 b_9^2 \quad (45)$$

The optimum temperature for the efficiency is then obtained:

$$T_{1,\eta} = \frac{-b_{12} - \sqrt{b_{12}^2 - 4b_{11}b_{13}}}{2b_{11}} \quad (46)$$

In a similar manner to the power maximization, Eq. (46) can be used to evaluate the optimum power output \dot{W}_η , Eq. (31), the optimum temperatures of the cycle, Eqs. (10), (13) and (14), and the rates of heat transfer, Eqs. (1) a (4). Expressions for the optimum entropy generation rate at maximum thermal efficiency condition $\dot{S}_{g,\eta}$ e for the maximum thermal efficiency η_{\max} are finally written as:

$$\dot{S}_{g,\eta} = \frac{\dot{Q}_{L,\eta}}{T_L} - \frac{\dot{Q}_{H,\eta}}{T_H} = \frac{\dot{Q}_{LC,\eta} + \dot{Q}_I}{T_L} - \frac{\dot{Q}_{HC,\eta} + \dot{Q}_I}{T_H} \quad (47)$$

$$\eta_{\max} = \frac{\dot{W}_\eta}{\dot{Q}_{H,\eta}} = \frac{\dot{W}_\eta}{\dot{Q}_{HC,\eta} + \dot{Q}_I} \quad (48)$$

5. RESULTS AND DISCUSSION

The relation between the dimensionless power output $\dot{W}/(\dot{C}_w T_H)$ and the thermal efficiency is showed in Fig. 2 to Fig. 5 varying different characteristic parameters of the cycle. From these graphs it is noticed that there is a single point where the power output is at its maximum and also a single point where the thermal efficiency is maximum, and in this latter case the power is slightly less than the maximum power output. Attention should be paid to the fact that the optimal region of operation is located between these two extreme points, because the operation points situated in the left of \dot{W}_{\max} provide lower values both in power output as well as in thermal efficiency than the points operating in the optimal region, which also ends up happening at points below η_{\max} . Therefore, it is in the region to the right of \dot{W}_{\max} and above η_{\max} , which is the optimal region of cycle operation, where the operation points show the highest values of power and efficiency

Fig. 2 presents the relation $\dot{W}/(\dot{C}_w T_H) \times \eta$ for some values of the reservoir temperature ratio T_H/T_L , showing that the increase of this factor leads to a considerable addition both in \dot{W}_{\max} as well as in η_{\max} . The influence of N_H and N_L in the $\dot{W}/(\dot{C}_w T_H)$ and η values is shower in Fig. 3, making clear the influence of these parameters in the cycle performance. The graphic also shows that the increase of N_H and N_L , when their values are closer to the unity, leads to a great increase in \dot{W}_{\max} and in η_{\max} . However, this becomes less evident each time this increase happens, making the improvement in the performance of the cycle less apparent for posterior additions in the values of these parameters.

Fig. 4 indicates the strong influence of the isentropic efficiencies in the maximum values that the cycle can achieve with respect to the power output and thermal efficiency, and that the increase in η_r leads to better results than the increase in η_c . The heat leakage is also analyzed in Fig 5, where it can be observed that the value of \dot{W}_{\max} is independent of \dot{C}_I and this parameter has only influence on the cycle efficiency.

Vitor Pereira Repinaldo, Santiago del Rio Oliveira, Vicente Luiz Scalon
 Optimization of a Brayton Cycle at Maximum Power Operating Condition and at Maximum Thermal Efficiency Operating Condition

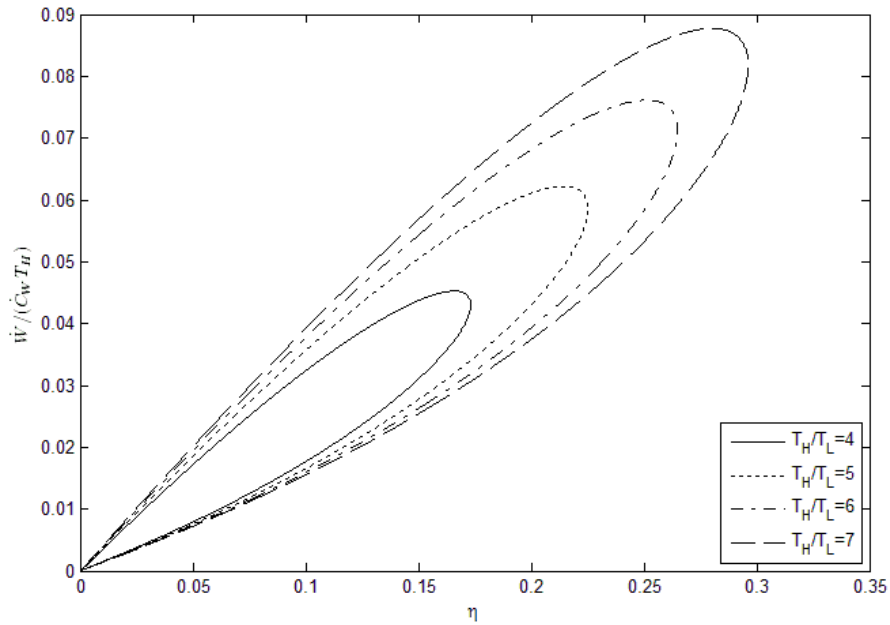


Figure 2. Variation of power output by the thermal efficiency for various values of T_H/T_L for constants $N_H = N_L = 1$, $\eta_r = \eta_c = 0.9$ and $\dot{C}_l/\dot{C}_w = 0.02$.

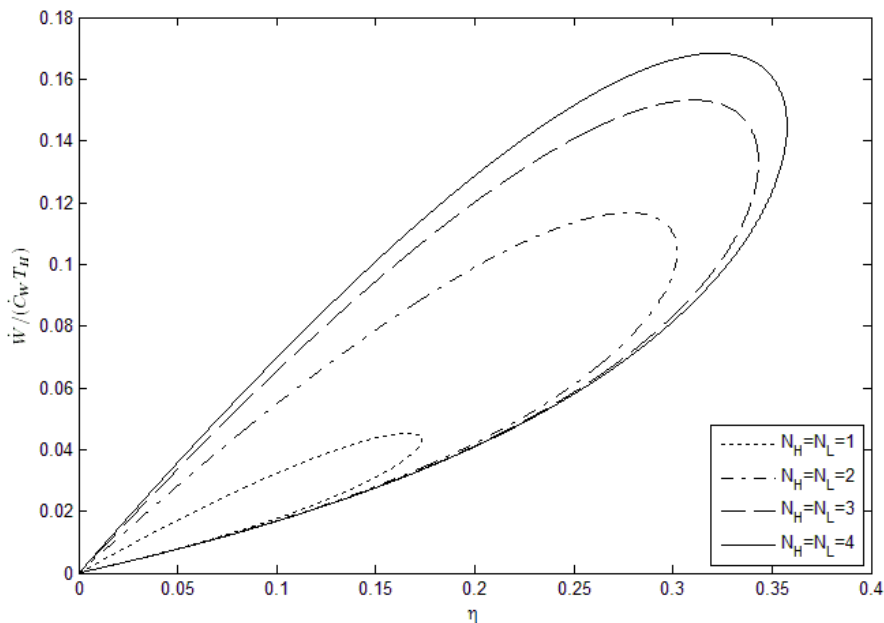


Figure 3. Variation of power output by the thermal efficiency for various values of N_H and N_L for constants $T_H/T_L = 4$, $\eta_r = \eta_c = 0.9$ and $\dot{C}_l/\dot{C}_w = 0.02$.

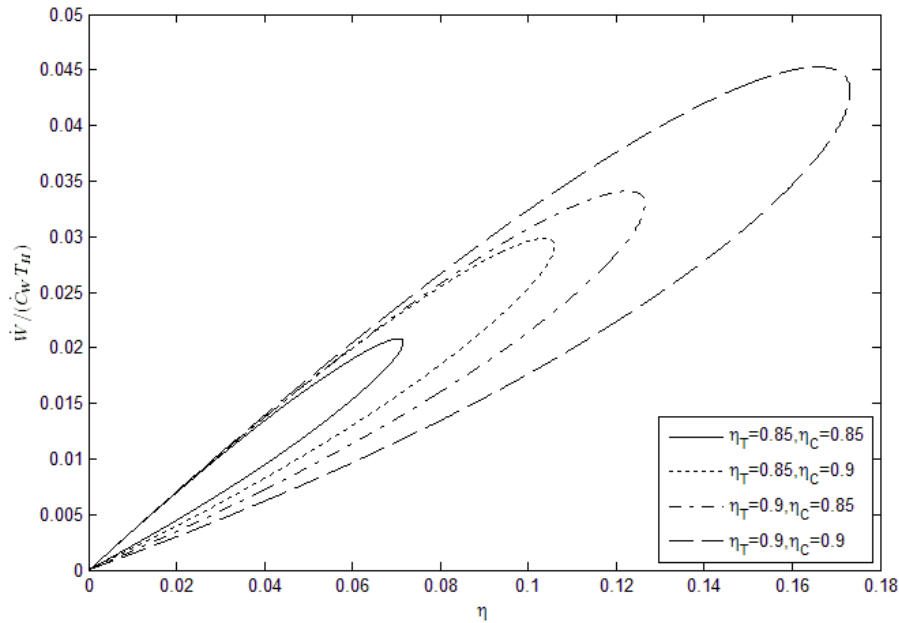


Figure 4. Variation of power output by the thermal efficiency for various values of η_T and η_c for constants $T_H/T_L = 4$, $N_H = N_L = 1$ and $\dot{C}_I/\dot{C}_W = 0.02$.

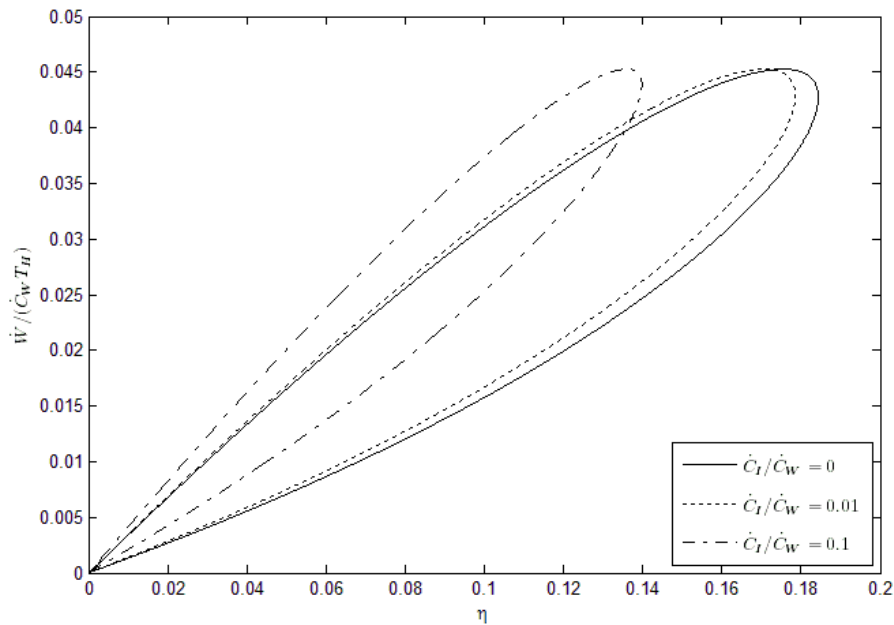
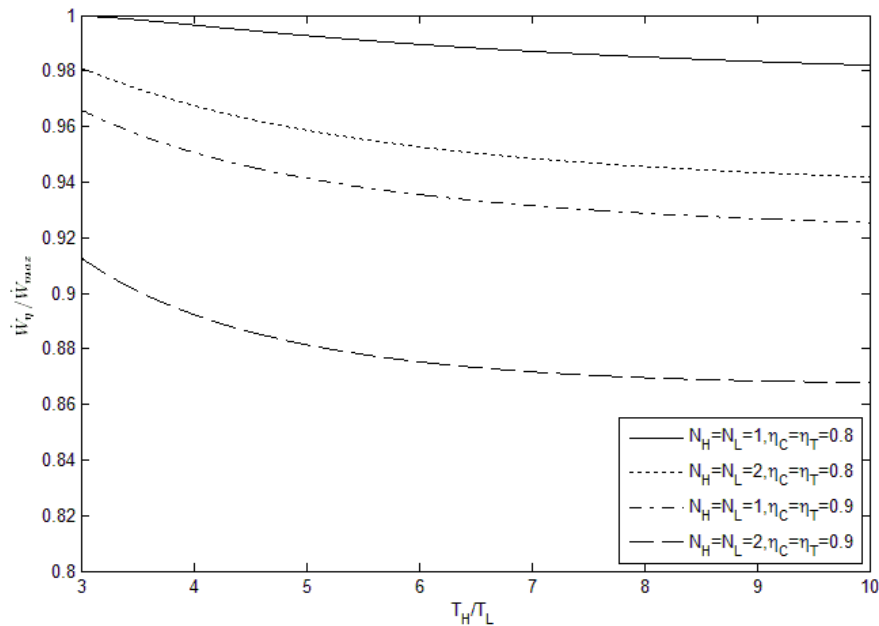
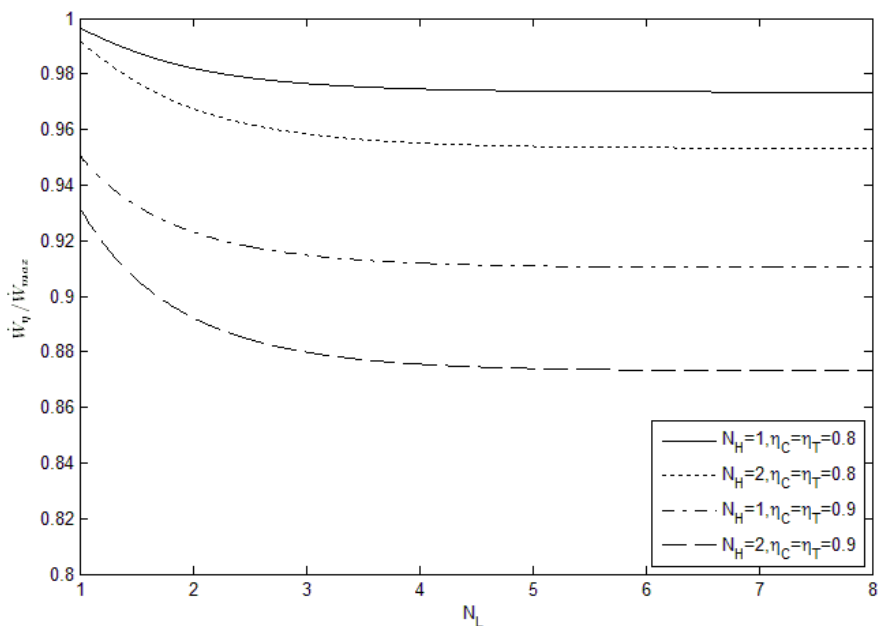


Figure 5. Variation of power output by the thermal efficiency for various values of \dot{C}_I/\dot{C}_W for constants $T_H/T_L = 4$, $N_H = N_L = 1$ and $\eta_T = \eta_c = 0.9$.

Vitor Pereira Repinaldo, Santiago del Rio Oliveira, Vicente Luiz Scalon
 Optimization of a Brayton Cycle at Maximum Power Operating Condition and at Maximum Thermal Efficiency Operating Condition



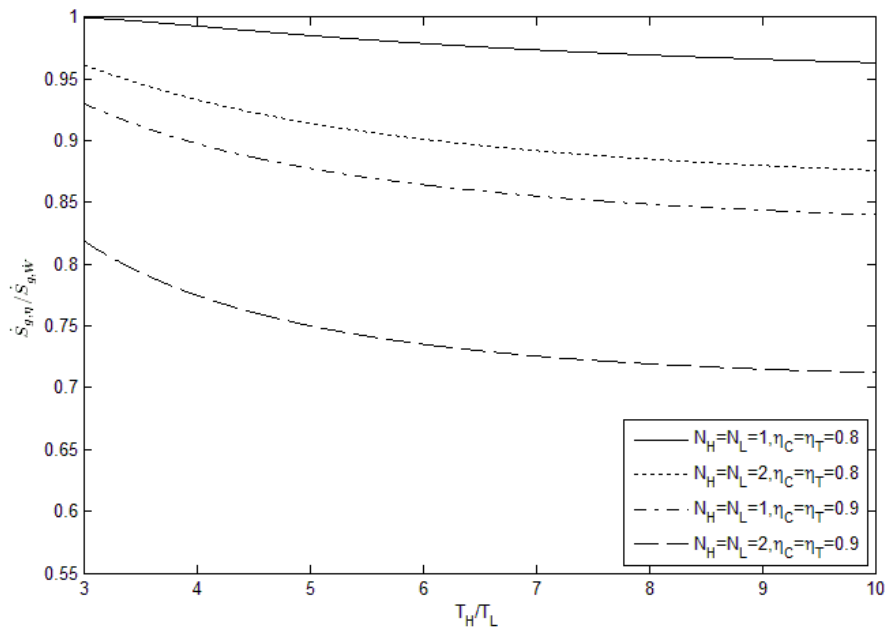
(a)



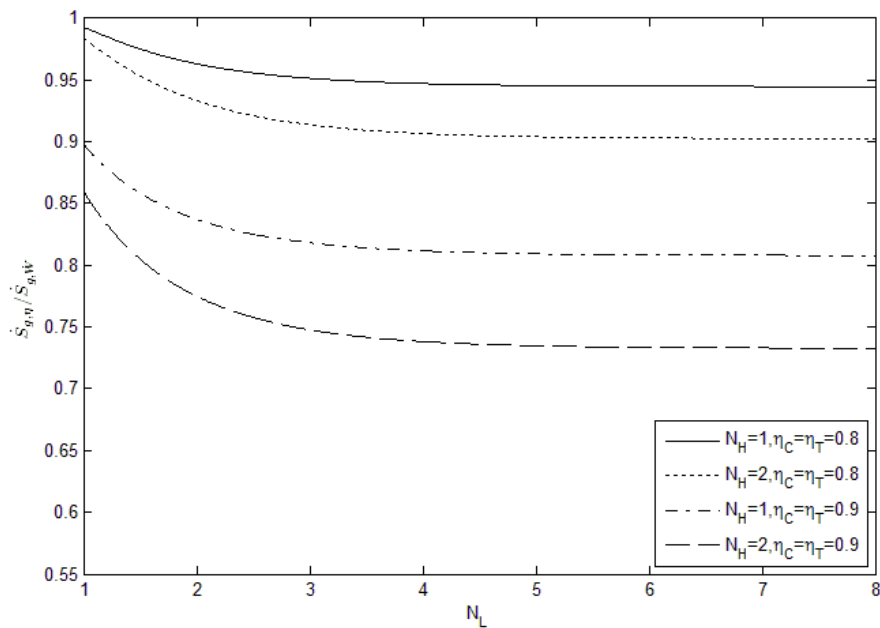
(b)

Figure 6. Ratio of the power output at maximum efficiency to the maximum power output with respect to (a) T_H/T_L and (b) N_L (when required the selected constants are $T_H/T_L = 4$, $N_H = N_L = 1$, $\eta_r = \eta_c = 0.9$ and $\dot{C}_i/\dot{C}_w = 0.02$).

The behavior of the ratio of the power output at maximum efficiency to the maximum power output, $\dot{W}_\eta/\dot{W}_{max}$, can be seen in Figs. 6(a) and 6(b) according to T_H/T_L and N_L , respectively. $\dot{W}_\eta/\dot{W}_{max}$ approaches the unity for lower values of N_H, N_L, η_r and η_c and $\dot{W}_\eta/\dot{W}_{max}$ approaches 85% when these parameters are increased. The difference between the powers under these two conditions is also highlighted when increased T_H/T_L .



(a)

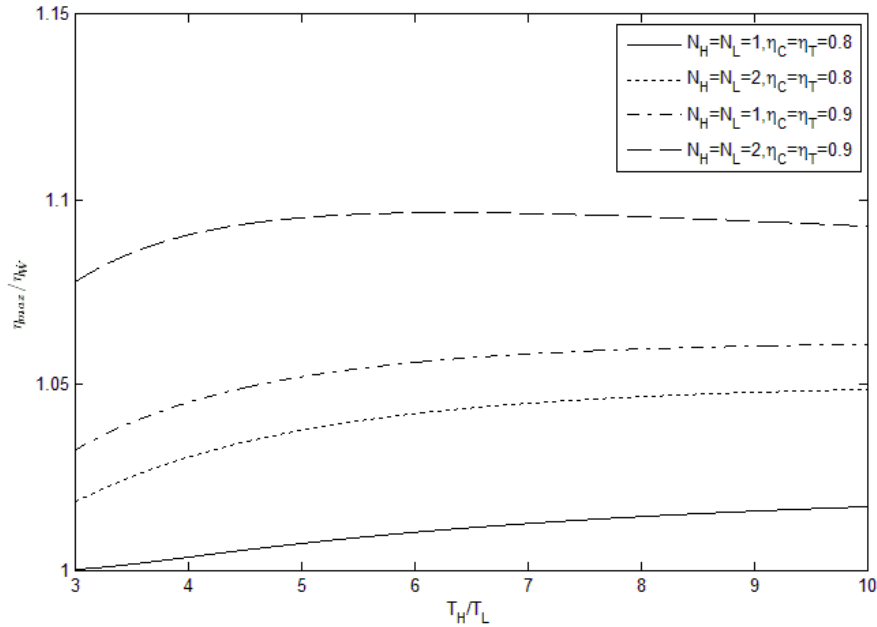


(b)

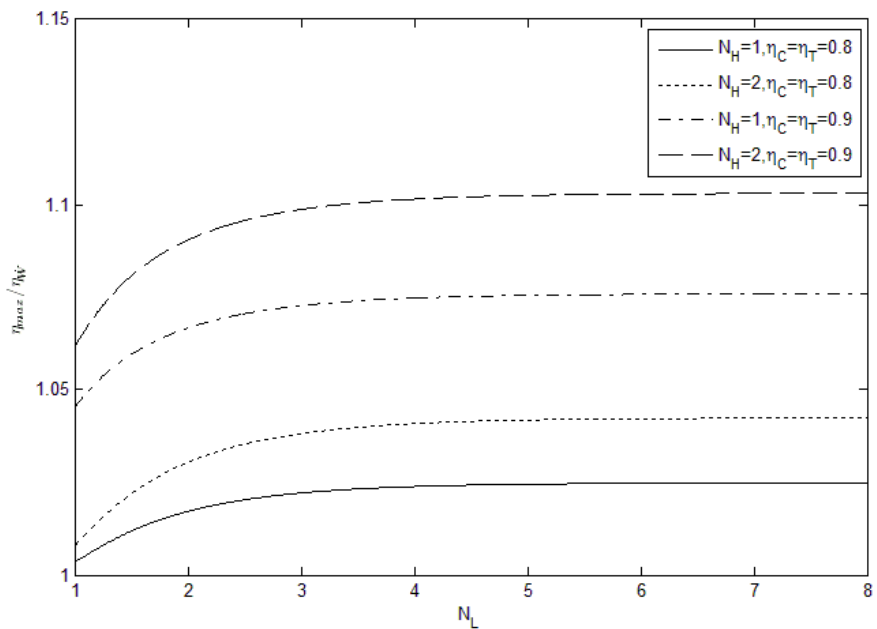
Figure 7. Ratio of the entropy generation rate at maximum efficiency to the entropy generation rate at maximum power output with respect to (a) T_H/T_L e (b) N_L (when required the selected constants are $T_H/T_L = 4$, $N_H = N_L = 1$, $\eta_T = \eta_c = 0.9$ and $\dot{C}_i/\dot{C}_w = 0.02$).

The ratio of the entropy generation rate at maximum efficiency to the entropy generation rate at maximum power, $\dot{S}_{g,\eta}/\dot{S}_{g,W}$, can be seen in Figs. 7(a) and 7(b) according to T_H/T_L and N_L , respectively. Similarly to $\dot{W}_\eta/\dot{W}_{\max}$, the difference between the performance of both optimizations becomes more evident for higher values of N_H, N_L, η_T, η_c and T_H/T_L . However, in this case, this difference comes close to 70% when these parameters suffer an increase. This

makes clear the ability of the thermal efficiency optimization to significantly reduce the value of \dot{S}_g , although with a small reduction in the power output as seen in Figs. 6(a) and 6(b).



(a)



(b)

Figure 8. Ratio of the maximum thermal efficiency to the thermal efficiency at maximum power output with respect to (a) T_H/T_L e (b) N_L (when required the selected constants are $\tau = 4$, $N_H = N_L = 1$, $\eta_T = \eta_C = 0.9$ and

$$\dot{C}_I/\dot{C}_W = 0.02).$$

Lastly, the ratio of the maximum thermal efficiency to the thermal efficiency at maximum power, η_{max}/η_W , can be seen in Figs. 8(a) and 8(b) as function of T_H/T_L and N_L , respectively. It can be observed the same behavior with respect to the parameters N_H, N_L, η_T, η_C and T_H/T_L of Figs. 3 and 4. It is noticed that the maximum efficiency proved

be able to reach a value approximately 10% greater than the efficiency of the cycle operating at maximum power, justifying the considerable loss in the power output indicated by the value $\dot{W}_\eta / \dot{W}_{\max} = 0,85$ in Fig. 6(a) e 6(b) under the same conditions.

6. CONCLUSIONS

The operation of Brayton cycle under maximum efficiency condition proved able to produce lower values of entropy generation rate and greater values of thermal efficiency, despite the considerable loss of power, when compared to a cycle operating at maximum power. Therefore, the ideal type of operation will always depend on the purpose of the project, which may seek greater efficiencies and lower entropy generation rates at the expense of greater power output, or get lower efficiencies and greater entropy generation rates aiming higher powers. However, what cannot be forgotten is that it will not be a single optimal point ideal for all cases, but a range of optimum operation that will provide the best performances for the cycle, being situated between the two optimal conditions presented in this paper. Thus, when it is wanted a greater power output the cycle must operate in the left part of this range closer to the point of maximum power leaving the region to the right when greater efficiencies are aimed. An example of the search for intermediate operating points within this optimum range can be found in works that propose the ecological optimization, where the goal is to find an intermediate point which represents the best compromise between a high power output and a low entropy generation rate.

7. REFERENCES

- Chen, J., 1994. "The maximum power output and maximum efficiency of an irreversible Carnot heat engine". *Journal of Physics D: Applied Physics*, Vol. 27, p. 1144.
- Chen, L., Sun, F. and Wu, C., 1997. "Influence of internal heat leak on the power versus efficiency characteristics of heat engines". *Energy Conversion and Management*, Vol. 38, p 1501.
- Chen, L., Zheng, J., Sun, F. and Wu, C., 2002. "Performance comparison of an endoreversible closed variable temperature heat reservoir Brayton cycle under maximum power density and maximum power conditions". *Energy Conversion and Management*, Vol. 43, p. 33.
- Curzon, F.L. and Ahlborn, B., 1975. "Efficiency of a Carnot engine at maximum power output". *American Journal of Physics*, Vol. 43, p. 22.
- Ibrahim, O. M., Klein, S. A. and Mitchell, J. W., 1991. "Optimum heat power cycles for specified boundary conditions". *ASME Journal of Engineering for Gas Turbines and Power*, Vol. 113, p 514.
- Sánchez-Orgaz, S., Medina, A. and Hernández, A. C., 2010. "Thermodynamic model and optimization of a multi-step irreversible Brayton cycle". *Energy Conversion and Management*, Vol. 51, p. 2134.
- Wu, C., 1988. "Power optimization of a finite-time Carnot heat engine". *Energy*, Vol. 13, p. 681.
- Wu, C., 1991. "Power optimization of a endoreversible Brayton gas heat engine". *Energy Conversion and Management*, Vol. 31, p. 561.
- Wu, C. and Kiang, R. L., 1991. "Power performance of a nonisentropic Brayton cycle". *ASME Journal of Engineering for Gas Turbines and Power*, Vol. 113, p. 501.
- Wu, C. and Kiang, R. L., 1992. "Finite-time thermodynamic analysis of a Carnot engine with internal irreversibility". *Energy*, Vol. 17, p. 1173.
- Zhang, W., Chen, L. and Sun, F., 2009. "Power and efficiency optimization for combined Brayton and inverse Brayton cycles". *Applied Thermal Engineering*, Vol. 29, p. 2885.
- Zhang, W., Chen, L. and Sun, F., 2012. "Energy performance optimization of combined Brayton and two parallel inverse Brayton cycles with regeneration before the inverse cycles". *Scientia Iranica*, Vol. 19, p. 1279.

8. RESPONSIBILITY NOTICE

The authors are the only responsible for the printed material included in this paper.